



## Coherent pattern and timing of the carbon isotope excursion and warming during Eocene Thermal Maximum 2 as recorded in planktic and benthic foraminifera

Lucy Stap, Lucas Lourens, and Arnold van Dijk

Faculty of Geosciences, Utrecht University, Budapestlaan 4, NL-3584 Utrecht, Netherlands  
(stap@geo.uu.nl)

Stefan Schouten

Department of Marine Organic Biogeochemistry, Royal Netherlands Institute for Sea Research,  
PO Box 59, NL-1790 AB Den Burg, Netherlands

Ellen Thomas

Center for the Study of Global Change, Department of Geology and Geophysics, Yale University,  
New Haven, Connecticut 06520-8109, USA

Also at Department of Earth and Environmental Sciences, Wesleyan University, Middletown,  
Connecticut 06459-0139, USA

[1] Eocene Thermal Maximum 2 (ETM2; ~53.7 Ma) occurred approximately 2 Myr after the Paleocene-Eocene Thermal Maximum (~55.5 Ma) and was characterized by a deep-sea warming of  $>3^{\circ}\text{C}$ , associated with massive release of carbon into the ocean-atmosphere system. We performed single-specimen stable isotope analyses of the planktic foraminiferal genera *Acarinina* (surface dweller) and *Subbotina* (thermocline dweller) from Ocean Drilling Program Sites 1265, 1267, and 1263 (Walvis Ridge, SE Atlantic Ocean) and compared high-resolution planktic and benthic stable isotope records to constrain the surface warming and the bathymetric pathway of the carbon isotope excursion during ETM2. Tests of the thermocline dweller *Subbotina* are absent from sediment deposited during the peak of ETM2. The *Acarinina* carbon and oxygen isotope records of Sites 1263, 1265, and 1267 are strikingly similar, despite some test recrystallization and large differences in burial depths. Sea surface temperature (SST) estimates based on  $\delta^{18}\text{O}$  isotope values of *Acarinina* indicate a SST increase of  $\sim 2^{\circ}\text{C}$ , significantly less than the  $>3^{\circ}\text{C}$  estimated for bottom water warming. The maximum negative carbon isotope excursion for *Acarinina* was  $\sim 1.7\text{‰}$ , slightly more than in the deep sea ( $\sim 1.4\text{‰}$ ). The planktic and benthic isotope records do not show time lags, indicating that during ETM2 the isotopically depleted carbon injected into the ocean-atmosphere system was rapidly mixed within all oceanic carbon reservoirs.

**Components:** 6000 words, 4 figures.

**Keywords:** hyperthermals; PETM; Eocene.

**Index Terms:** 3344 Atmospheric Processes: Paleoclimatology (0473, 4900); 0473 Biogeosciences: Paleoclimatology and paleoceanography (3344, 4900); 4948 Paleocyanography: Paleocene/Eocene thermal maximum.

**Received** 19 February 2010; **Revised** 16 August 2010; **Accepted** 14 September 2010; **Published** 20 November 2010.

Stap, L., L. Lourens, A. van Dijk, S. Schouten, and E. Thomas (2010), Coherent pattern and timing of the carbon isotope excursion and warming during Eocene Thermal Maximum 2 as recorded in planktic and benthic foraminifera, *Geochem. Geophys. Geosyst.*, 11, Q11011, doi:10.1029/2010GC003097.



## 1. Introduction

[2] The early Eocene warm period (56–49 Ma) was characterized by short (~100 kyr) intervals of extreme warming, called hyperthermals or Thermal Maxima, of which the most extreme was the Paleocene-Eocene Thermal Maximum (PETM; ~55.5 Ma). Eocene Thermal Maximum 2 (ETM2; ~53.7 Ma) was a distinct period of global warming approximately 2 Myr after the PETM [Lourens *et al.*, 2005; Stap *et al.*, 2009]. High-resolution benthic stable isotope ( $\delta^{18}\text{O}$  and  $\delta^{13}\text{C}$ ) records from the southeastern Atlantic show that deep-sea temperatures rose by  $>3^\circ\text{C}$  during ETM2, with a carbon isotope excursion (CIE) of  $-1.4\text{‰}$  [Stap *et al.*, 2010], both approximately half the PETM magnitude. However, the  $\delta^{13}\text{C}$  change of the exogenic carbon pool was related to warming in a similar way during both events, despite the much more gradual onset of ETM2 [Stap *et al.*, 2010].

[3] Stable isotope records of planktic foraminiferal species from deep-sea sites in the Southern Ocean show a stratigraphic offset reflecting a time lag between the  $\delta^{13}\text{C}$  records from the mixed layer and those of the thermocline and deep sea during the onset of the PETM [Thomas *et al.*, 2002; Zachos *et al.*, 2007]. A similar study has not yet been performed for ETM2, and only a relatively low resolution planktic stable isotope record is available for Ocean Drilling Program (ODP) Site 1263 [Lourens *et al.*, 2005]. In this study we present  $\delta^{13}\text{C}$  and  $\delta^{18}\text{O}$  records from ODP Site 1265 at high resolution and from Site 1267 at lower resolution, based on single-test measurements of surface and thermocline dwelling planktic foraminiferal taxa across ETM2. Comparison of the planktic stable isotope results with multiple-specimen benthic foraminiferal isotope records from the same samples [Stap *et al.*, 2010] are used to constrain the surface warming and the bathymetric pathway of the carbon isotope excursion during ETM2. In addition, we used the organic-based TEX<sub>86</sub> proxy [Schouten *et al.*, 2002] to independently estimate sea surface temperature (SST) during peak ETM2 conditions.

## 2. Materials and Methods

### 2.1. Sites and Location

[4] ODP Leg 208 recovered sediments deposited during ETM2 at 5 sites along a ~2 km depth transect on the northeastern flank of Walvis Ridge, southeastern Atlantic Ocean [Zachos *et al.*, 2004].

Samples were used from ODP Sites 1263 (28°31.98'S, 02°46.77'E, 2717 m water depth), 1265 (28°50.10'S, 02°38.35'E, 3060 m water depth), and a lower-resolution record for Site 1267 (28°05.88'S, 01°42.66'E, 4355 m water depth). ETM2 is marked by a carbonate dissolution horizon in the Walvis Ridge sediments, termed the Elmo horizon [Lourens *et al.*, 2005]. Depths in core across the dissolution intervals at the 3 sites were placed on a common relative age scale [Stap *et al.*, 2009], which allows comparison with the lower-resolution planktic stable isotope data of Site 1263 [Lourens *et al.*, 2005].

### 2.2. Samples and Processing

[5] High-resolution stable isotope ( $\delta^{13}\text{C}$  and  $\delta^{18}\text{O}$ ) records were generated using individual planktic foraminiferal tests across ETM2 at Sites 1265 and 1267. Single-specimen isotopic analyses were carried out on the surface-dwelling, photosymbiont-bearing genus *Acarinina* and the thermocline-dwelling genus *Subbotina* [D'Hondt and Zachos, 1998]. Specimens were selected in a narrow size range, 300–355  $\mu\text{m}$ , to minimize ontogenic variability. Approximately five specimens from both species per sample were selected for stable isotope analysis. Scanning electron micrographs (SEM) document the preservation state of the planktic foraminifers.

### 2.3. Isotope Analyses

[6] Prior to analysis, specimens were ultrasonically cleaned in methanol for 10 s to remove adhering particles. Stable isotope analyses were performed on a CARBO-KIEL automated carbonate preparation device linked online to a Finnigan MAT253 mass spectrometer at Utrecht University. Calibration to the international standard NBS-19 and in-house standard Naxos shows that analytical precision was better than 0.02‰ and 0.08‰ for  $\delta^{13}\text{C}$  and  $\delta^{18}\text{O}$ , respectively. All values are reported in standard delta notation ( $\delta$ ) relative to VPDB (Vienna Pee Dee Belemnite).

### 2.4. TEX<sub>86</sub> Analysis

[7] One composite sediment sample (35 g) that covered the entire Elmo horizon of Site 1263 was analyzed for TEX<sub>86</sub> [Schouten *et al.*, 2002]. The powdered and freeze-dried sediment was extracted with dichloromethane (DCM)/methanol (MeOH) (9:1, v/v) using the accelerated solvent extraction technique (Dionex). The extract was separated in apolar and polar fractions using column chro-

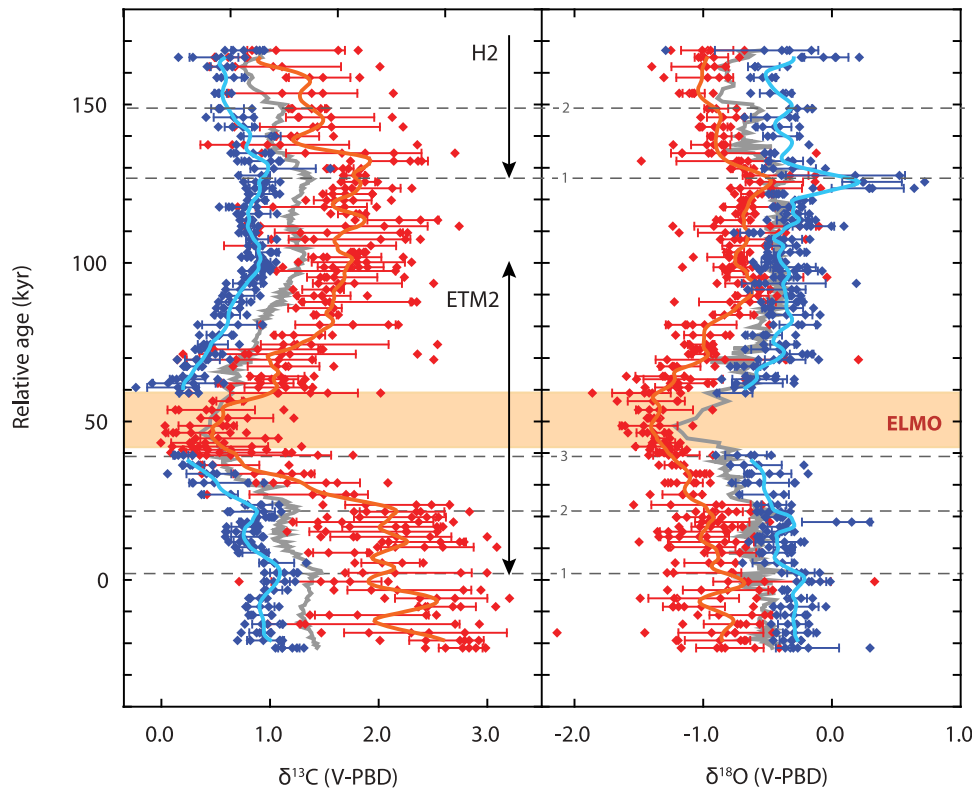


**Figure 1.** Single-specimen oxygen and carbon isotope data for Site 1265, Leg 208 Walvis Ridge. Lines indicate a 4 kyr moving average. Analyses were carried out on the surface dweller *Acarinina* (red diamonds) and thermocline dweller *Subbotina* (blue diamonds) from the 300–355  $\mu\text{m}$  fraction. Bars across sample horizons show the standard deviation within a sample. Previously published bulk isotope data (in gray) are from Stap *et al.* [2009]. The dashed horizontal lines indicate the transitions (1–3) in carbonate dissolution, coupled to rapid depletions in bulk carbonate carbon isotope values during the onset of ETM2 and H2 according to Stap *et al.* [2009]. Indicated in light orange is the Elmo horizon [Lourens *et al.*, 2005].

matography. The polar fraction, containing glycerol dialkyl glycerol tetraethers was analyzed using high-performance liquid chromatography/atmospheric pressure positive ion chemical ionization mass spectrometry (HPLC/APCI-MS), using an Agilent 1100 series LC/MSD SL and a Prevail Cyano column (2.1  $\times$  150 mm, 3 mm; Alltech), maintained at 30°C [Schouten *et al.*, 2007].

### 3. Results

[8] Despite the use of a narrow size range of individual planktic specimens to minimize ontogenic variability, the stable isotope record of *Acarinina* shows a wide range of values within each sample, corresponding to average standard deviations of  $\delta^{13}\text{C}$  and  $\delta^{18}\text{O}$  of 0.4‰ and 0.2‰, respectively. The average standard deviations for  $\delta^{13}\text{C}$  and  $\delta^{18}\text{O}$  of *Subbotina* from each sample are significantly lower ( $\sim$ 0.1‰). The large scatter in the *Acarinina* record is comparable to the scatter in

the single-test record across the PETM at Bass River [John *et al.*, 2008], and in single-test records of modern-day surface-dwelling foraminifera [e.g., Schiffelbein and Hills, 1984], and might be due to a variety of factors related to seasonal variability. *Subbotina* might have been able to adjust its depth of calcification in response to environmental changes, possibly following isotherms and/or the nutricline, whereas the vertical motion of *Acarinina* was probably more limited, because this genus probably relied on photosymbionts, and therefore must have remained within the euphotic zone [Handley *et al.*, 2008]. A shallower habitat of *Acarinina* versus *Subbotina* within the euphotic zone is consistent with its heavier  $\delta^{13}\text{C}$  and lighter  $\delta^{18}\text{O}$  average values throughout the studied interval.

[9] Average  $\delta^{18}\text{O}$  values prior to ETM2 are about  $-0.9\text{‰}$  and  $-0.4\text{‰}$  for *Acarinina* and *Subbotina*, respectively. Oxygen isotopes ratios of *Acarinina* decrease gradually by  $\sim$ 0.5‰ across the onset of ETM2, followed by an increase of  $\sim$ 0.8‰ over the

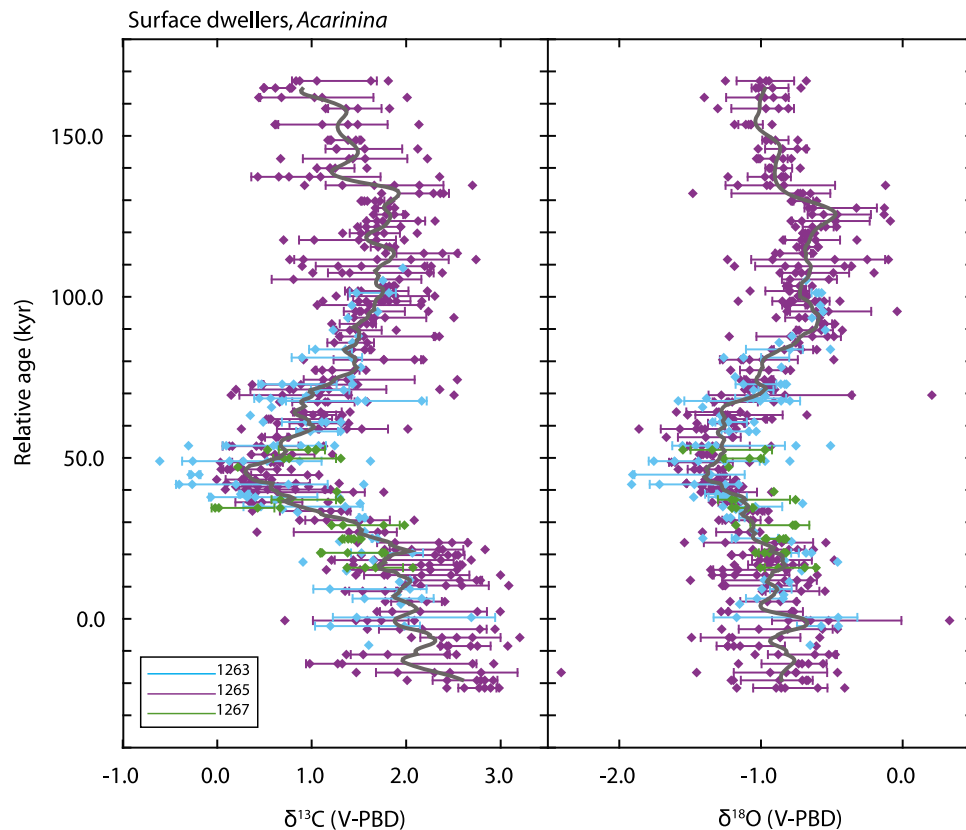


**Figure 2.** Comparison of the carbon and oxygen *Acarinina* records of Site 1265 with those of Site 1267 (this study) and Site 1263 [Lourens *et al.*, 2005].

recovery phase. The changes in the  $\delta^{18}\text{O}$  record of *Acarinina* are similar to those in the lower-resolution records of Sites 1263 [Lourens *et al.*, 2005] and 1267 (Figure 2). Changes in the oxygen isotope values of *Subbotina* are small, partly because of the absence of this genus within the Elmo horizon. However, the decrease in the  $\delta^{18}\text{O}$  record of *Subbotina* during the first part of the onset of ETM2 is also minor (0.2‰).

[10] The  $\delta^{13}\text{C}$  record of *Subbotina* closely matches the bulk  $\delta^{13}\text{C}$  record, and has a systematic offset of approximately  $-0.3\text{‰}$ . The onset of ETM2 is characterized by three precession-paced transitions in carbonate dissolution (gray lines in Figure 1), coupled to rapid carbon isotope depletions in bulk carbonate [Stap *et al.*, 2009] and *Subbotina*. (See Data Set S1 for single-specimen oxygen and carbon isotope data for Site 1265.)<sup>1</sup> The first and second transitions (marked by numbers 1 and 2 in Figure 1) comprise a combined CIE of  $>-0.8\text{‰}$ . The complete extent of the CIE is not recorded by *Subbotina*,

because specimens of this genus are absent within the Elmo horizon (Figure 1). The CIE in *Acarinina* is  $\sim-1.7\text{‰}$ , with the largest decrease during the second transition at Site 1265 (Figure 1). The CIE in *Acarinina* is larger than in *Subbotina* in the interval following transition 2, where both genera are present. Thus, during ETM2, the vertical  $\delta^{13}\text{C}$  gradient between bulk values and *Acarinina* values decreased slightly.

[11] Comparison of our carbon isotope results of *Acarinina* from Site 1265 and 1267 with those of the nearby Site 1263 [Lourens *et al.*, 2005] indicates an almost identical pattern at all three sites, although values from specimens within the Elmo horizon are slightly lighter at Site 1263 (Figure 2). The single-test stable isotope measurements of *Subbotina* and *Acarinina* have  $\delta^{13}\text{C}$  values intermediate between preevent values and peak CIE values during the onset of ETM2 (Figure 1), intermediate between preevent values and peak CIE values during the onset of ETM2 (Figure 1), whereas such intermediate values have not been seen during the preevent to event transition of the PETM [Thomas *et al.*, 2002].

<sup>1</sup>Auxiliary materials are available at <ftp://ftp.agu.org/apend/gc/2010gc003097>.



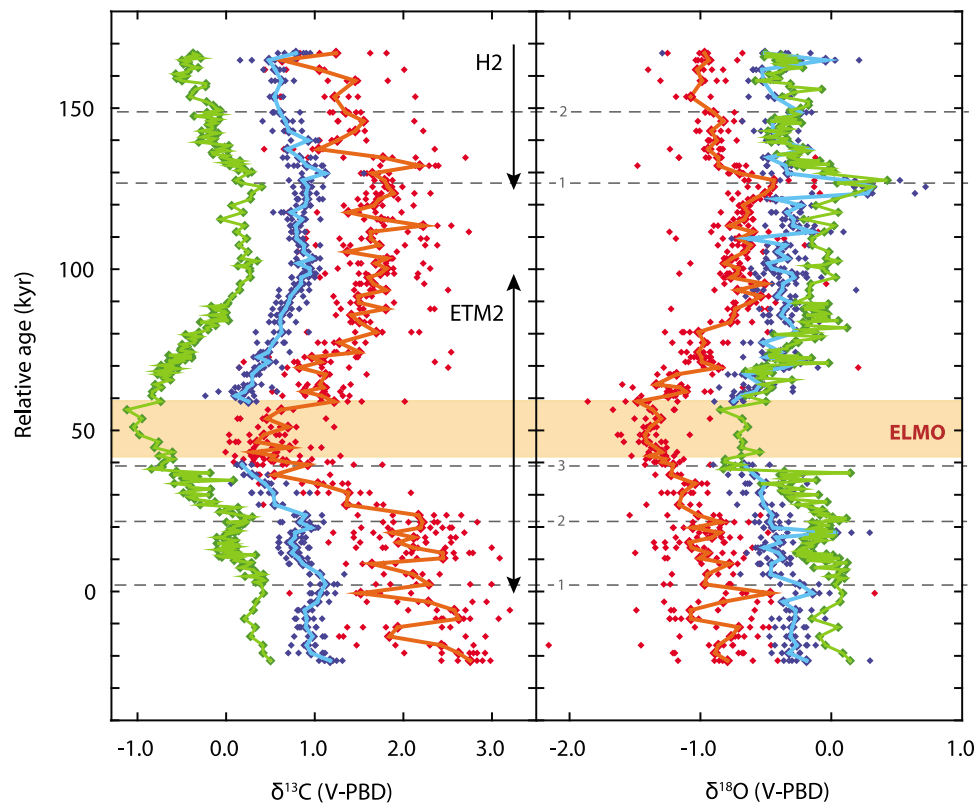


**Figure 3.** Comparison of the evolution of the carbon and oxygen isotopes of surface-dwelling genus *Acarinina* (red diamonds), thermocline-dwelling genus *Subbotina* (blue diamonds), and previously measured benthic foraminifera [Stap et al., 2010] (green diamonds) plotted against relative age. Lines represent average values. Grey lines indicate the transitions in carbonate dissolution, coupled to rapid depletions in bulk carbonate carbon isotope values during the onset of ETM2 and H2 according to Stap et al. [2009]. Indicated in light orange is the Elmo horizon [Lourens et al., 2005].

[12] A second, but smaller CIE (termed H2) occurred approximately 100 kyr after ETM2 at ~128 ka [Cramer et al., 2003], and is associated with a deep-sea temperature increase of ~2°C and reduced carbonate content [Stap et al., 2009]. We have measured only the onset of H2 in Site 1265. The magnitudes of the H2 CIE excursions are ~-0.7‰ and ~-0.3‰ for *Acarinina* and *Subbotina*, respectively. In contrast to ETM2, *Subbotina* remains present during H2, so that we can observe that the vertical  $\delta^{13}\text{C}$  gradient between *Subbotina* and *Acarinina* values decreased slightly. The  $\delta^{18}\text{O}$  record of *Acarinina* reflects ~-0.2‰ depletion during H2. The records of *Subbotina*, *Acarinina* and benthic foraminifera show a short maximum in  $\delta^{18}\text{O}$  values prior to H2, at ~123 kyr, which is not accompanied by an increase in  $\delta^{13}\text{C}$  values (Figure 3).

[13] The  $\text{TEX}_{86}$  value for the Elmo composite sample of Site 1263, was 0.64. We applied the core top calibration equation from Kim et al. [2010] to translate the  $\text{TEX}_{86}$  value to an estimate of mean

annual sea surface temperature which yields a temperature estimate of ~25°C, with a calibration error of 2.5°C.

## 4. Discussion

### 4.1. Secondary Overprint

[14] To assess the significance of diagenesis on the stable isotope records, we will discuss possible effects during three successive stages: (1) calcification, (2) early diagenesis, and (3) diagenesis after burial. A massive and rapid injection of  $\text{CO}_2$  into the ocean-atmosphere system during ETM2 should have caused a decrease in seawater pH and  $[\text{CO}_3^{2-}]$  and influence thereby the  $\delta^{13}\text{C}$  and  $\delta^{18}\text{O}$  composition of the planktic foraminifera [Spero et al., 1997]. Modeling studies for the PETM (using various carbon input scenarios of 2000–5000 Gt C) show that the carbonate ion effect could decrease the changes in  $\delta^{13}\text{C}$  of planktic foraminifera by up

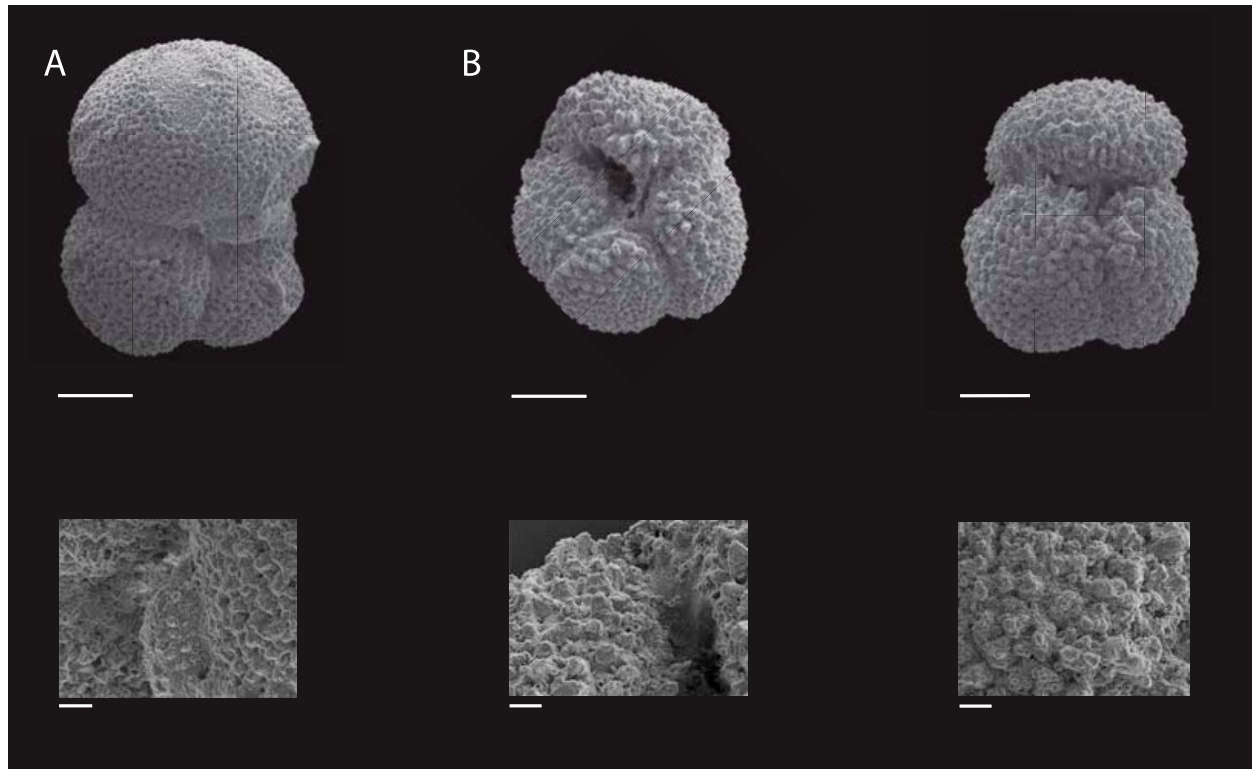


**Figure 4.** Scanning electron microscope (SEM) micrographs of test wall of unsonicated specimens of *Subbotina* spp. and *Acarinina* spp. of Site 1265. Scale bars are 100  $\mu\text{m}$  for the main images and 20  $\mu\text{m}$  for the detailed SEM images of the wall structure.

to 2.1 and  $\delta^{18}\text{O}$  by up to 0.7‰ [Uchikawa and Zeebe, 2010]. This effect could even be larger for benthic foraminifera, (up to 2.8 and 0.9 for  $\delta^{13}\text{C}$  and  $\delta^{18}\text{O}$ , respectively).

[15] The amount of carbon released during ETM2 (~900–2400 Gt C) is probably about half of that released during the PETM [Lourens *et al.*, 2005], which may imply that the  $\delta^{13}\text{C}$  and  $\delta^{18}\text{O}$  values of the planktic and benthic foraminifers could be damped by ~1‰ and ~0.4‰, respectively, corresponding to an error in paleotemperature estimate of more 1.5°C. Uchikawa and Zeebe [2010] assumed, however, a release rate of carbon over 5 kyr during the PETM, while for ETM2, the release rate was ~20 kyr [Stap *et al.*, 2009], causing the effect of ocean acidification to be less rapid and severe and possibly a lesser effect on the carbon and oxygen isotope values. Nevertheless, it seems likely that the observed shifts in  $\delta^{13}\text{C}$  and  $\delta^{18}\text{O}$  during ETM2 and H2 underestimate the true excursion by a few tenths of a per mille due to a decrease in seawater pH and  $[\text{CO}_3^{2-}]$ .

[16] The severe  $\text{CaCO}_3$  weight % loss within the Elmo horizon of ~90% to ~40% at the Walvis Ridge sites indicates that up to 96% of the total

carbonate flux was dissolved within the water column or during sedimentation [Stap *et al.*, 2009], probably due to shoaling of the lysocline and CCD. Hence the planktonic foraminiferal record may well be biased by preferential dissolution. An abrupt decrease in abundance or absence of *Subbotina* (>125  $\mu\text{m}$ ) during the peak CIE is observed at many PETM localities [Kelly *et al.*, 1998; Arenillas *et al.*, 1999; Kelly *et al.*, 2005; Luciani *et al.*, 2007; Petrizzo, 2007], and this genus may be more susceptible to dissolution [Petrizzo, 2007; Petrizzo *et al.*, 2008; Nguyen *et al.*, 2009].

[17] Partial dissolution studies on present-day planktic foraminifera have shown that the carbon and oxygen isotope values may increase by ~0.2‰, as shown for the deep-dwelling foraminiferal species *Neoglobobulimina pachyderma* [Hönisch, 2002]. In contrast, the isotopic composition of the surface dweller *Globigerinoides sacculifer* seems to be insensitive to partial dissolution [Hönisch, 2002]. The more dampened isotopic signature of ETM2 in *Subbotina* as compared to *Acarinina* could thus, to some extent, be due to partial dissolution. Scanning electron micrographs (Figure 4) show that tests of *Subbotina* and *Acarinina* are recrystallized. This



micrometer-scale diagenetic alteration may result in heavier  $\delta^{18}\text{O}$  values (i.e., lower temperatures) [Pearson *et al.*, 2001; Sexton *et al.*, 2006]. Nevertheless, paleoreconstructions on relatively short time scales are less compromised [Pearson *et al.*, 2001; Sexton *et al.*, 2006]. Using a numerical model, Schrag *et al.* [1995] estimated that SST values might be underestimated by 1–4°C due to burial diagenesis on bulk carbonate  $\delta^{18}\text{O}$  for Walvis Ridge DSDP Site 525 (close to our sites) However, despite their widely different burial depths [Lourens *et al.*, 2005], the *Acarinina*  $\delta^{18}\text{O}$  records of Sites 1263, 1265 and 1267 are strikingly similar, suggesting that burial diagenesis likely played a minor role.

## 4.2. Sea Surface Temperatures Changes During ETM2

[18] The oxygen isotope signal of planktonic foraminifers depends primarily on temperature and the isotopic composition of seawater ( $\delta^{18}\text{O}_{\text{sw}}$ ). During the early Eocene, the net evaporation over the southeastern Atlantic was probably more intense than today, and as a consequence, surface water salinities may have been as much as 2 ppt higher than at present [Roberts *et al.*, 2009]. Modeling experiments for the ice-free world of the early Paleogene suggested that surface  $\delta^{18}\text{O}_{\text{sw}}$  values may have been  $\sim -0.25\text{‰}$  (SMOW) in the eastern part of the South Atlantic Ocean [Roberts *et al.*, 2009], assuming that the surface  $\delta^{18}\text{O}_{\text{sw}}$  value was 0.7‰ heavier than the  $\delta^{18}\text{O}_{\text{sw}}$  value of  $-0.98\text{‰}$  (SMOW) generally assumed for the deep sea [Stap *et al.*, 2010]. Today, the  $\delta^{18}\text{O}_{\text{sw}}$  difference between surface and deep waters in the SE Atlantic Ocean may increase up to  $\sim 1.5\text{‰}$  during the summer months [Pierre *et al.*, 1991; Ostlund *et al.*, 1987], so we consider the  $\Delta\delta^{18}\text{O}_{\text{sw}}$  of 0.7‰ used in this study as a minimum value. Application of the paleotemperature equation of Erez and Luz [1983]:  $T^{\circ}\text{C} = 16.998 - 4.52 (\delta^{18}\text{O}_{\text{cc}} - \delta^{18}\text{O}_{\text{sw}}) + 0.028 (\delta^{18}\text{O}_{\text{cc}} - \delta^{18}\text{O}_{\text{sw}})^2$ , where 0.27‰ has been subtracted from  $\delta^{18}\text{O}_{\text{sw}}$  to correct between SMOW and PDB scales [Hut, 1987], implies that pre-ETM2 SSTs were about  $\sim 19^{\circ}\text{C}$  and thermocline temperatures  $\sim 16.5^{\circ}\text{C}$  at the Walvis Ridge sites. The decrease in *Acarinina*  $\delta^{18}\text{O}$  values of  $\sim 0.5\text{‰}$  during ETM2 suggests that SSTs rose to  $\sim 21^{\circ}\text{C}$ , assuming no change in  $\delta^{18}\text{O}_{\text{sw}}$ .

[19] In comparison, the  $\text{TEX}_{86}$ -based SST estimate from the Elmo horizon of Site 1263 yields a  $\sim 4^{\circ}\text{C}$  higher temperature than the  $\delta^{18}\text{O}$ -based SST estimate. Assuming that our adopted  $\delta^{18}\text{O}_{\text{sw}}$  values of  $\sim -0.25\text{‰}$  is correct, a likely explanation for this

offset could be the secondary overprint of the planktic foraminifers and effect of pH as discussed above, which can potentially lower our  $\delta^{18}\text{O}$ -based SST estimate by up to  $2^{\circ}\text{C}$ .

[20] Interestingly, the  $\text{TEX}_{86}$ -based SST value of  $\sim 25^{\circ}\text{C}$  is far lower than that reconstructed (also using the  $\text{TEX}_{86}$ ) for the high southern latitudes during the early Eocene, i.e.,  $>30^{\circ}\text{C}$  [Bijl *et al.*, 2009; Hollis *et al.*, 2009]. In present-day upwelling areas, the production of Crenarchaeota seems to occur at a greater depth, causing cold-biased  $\text{TEX}_{86}$ -based temperatures [Huguet *et al.*, 2007; Kim *et al.*, 2008; Lee *et al.*, 2008]. The relatively low  $\text{TEX}_{86}$ -based SST at Site 1265 could suggest that the Walvis Ridge Sites were near an upwelling zone [Zachos *et al.*, 1994], which may have caused a seasonal bias of the  $\text{TEX}_{86}$  and  $\delta^{18}\text{O}$ -based SST estimates.

[21] Despite these uncertainties in absolute temperature estimates and paleoceanographic inferences, the oxygen isotopes of planktic foraminifers may place valuable constraints on the trends and relative changes in temperature during ETM2 as compared to those during the PETM [Zachos *et al.*, 2003; Tripathi and Elderfield, 2004]. The maximum sea surface warming of  $\sim 2^{\circ}\text{C}$ , as derived from oxygen isotope values of *Acarinina* during ETM2, is significantly smaller than the coeval 3–4°C warming in the deep sea found at the same site [Stap *et al.*, 2010], and the SST increase of 3–5°C in the Arctic [Sluijs *et al.*, 2009]. Possibly, the net evaporation in the region may have been larger during ETM2 than before and after the event, enhancing the surface  $\delta^{18}\text{O}_{\text{sw}}$  values. Correcting the surface  $\delta^{18}\text{O}_{\text{sw}}$  by  $\sim 0.3\text{‰}$  would lead to a SST increase of 3–4°C. Such a scenario parallels temperature reconstructions of the PETM for some subtropical sites [Thomas *et al.*, 1999; Zachos *et al.*, 2003; Tripathi and Elderfield, 2004].

## 4.3. Magnitude of the CIE and Rate of Carbon Emission During ETM2

[22] The maximum CIE recorded in *Acarinina* of  $\sim -1.7\text{‰}$  was slightly larger than the  $\sim -1.4\text{‰}$  shift in benthic foraminifera [Stap *et al.*, 2010]. During the onset of ETM2, a reduced  $\delta^{13}\text{C}$  gradient started to develop between *Acarinina* and *Subbotina*, benthic foraminifera and bulk values (Figures 1 and 3). The  $\delta^{13}\text{C}$  of planktic foraminifera is expected to primarily reflect the  $\delta^{13}\text{C}_{\text{DIC}}$  of the seawater, but the  $\delta^{13}\text{C}$  of planktic foraminifera commonly deviates from the  $\delta^{13}\text{C}_{\text{DIC}}$  of seawater in which they calcify





[e.g., Kroon and Ganssen, 1989; Spero, 1992] because of vital effects [Spero, 1992; Spero et al., 1997; Bemis et al., 2000]. These effects are considered to be constant throughout the studied interval, since the standard deviations for both species remained largely the same. The reduced  $\delta^{13}\text{C}$  gradient between the surface (*Acarinina*) and deeper waters (*Subbotina* and bulk) could therefore reflect a decline in the efficiency of the biological pump or increased vertical mixing, as suggested for the PETM [Kennett and Stott, 1991; Zachos et al., 2007]. As discussed above, these inferences are complicated, however, by the fact that the isotopic composition of surface and thermocline dwellers could also reflect (1) changes in the  $[\text{CO}_3^{2-}]$  of the seawater, which may affected the  $\delta^{13}\text{C}$  composition of the various species differently [Spero et al., 1997], (2) secondary recrystallization during diagenesis [Pearson et al., 2001], or (3) seasonal effects.

[23] Giving the uncertainties in determination of the significance of the secondary overprint, seasonal effects may also have resulted in the reduced  $\delta^{13}\text{C}$  gradient between the surface and deep-dwelling species. With regard to the seasonal effects, we may consider that the symbiont-bearing *Acarinina* thrived in the surface waters during the more oligotrophic, well-stratified, warm water (summer) season of the year, whereas the “deeper-dwelling” *Subbotina* specimens and nannofossils calcified during the higher-productivity seasons characterized by colder waters, such as the spring or autumn blooms, due to enhanced mixing. The decreased  $\delta^{13}\text{C}$  gradient found in the surface ocean at Walvis Ridge during ETM2 may therefore indicate that summer productivity decreased, causing relatively depleted surface water  $\delta^{13}\text{C}_{\text{DIC}}$  values, whereas the high-productivity seasons became even more productive, causing enriched subsurface  $\delta^{13}\text{C}_{\text{DIC}}$  values (Figure 2). Alternatively, the *Acarinina* could have shifted their growth season toward the spring bloom during ETM2, especially within the Elmo horizon, possibly because temperatures were too high for this species. The decreased  $\delta^{13}\text{C}$  gradient could then be caused by mixing during the spring bloom. Such a scenario may also explain the small temperature increase of the *Acarinina*'s during ETM2, since they could record spring temperatures during the course of ETM2.

[24] Single-specimen stable isotope investigations of the onset of the PETM at Sites 690 and 689 in the Southern Ocean show that the thermocline dwelling planktic and deep-sea benthic foraminiferal species stratigraphically lag the CIE of the

mixed layer species by ~5 to 10 kyr, [Thomas et al., 2002; Zachos et al., 2007]. Hypotheses to explain this offset include lags in the propagation of injected carbon from the atmosphere to the surface and deep oceans [Thomas et al., 2002; Zachos et al., 2007], as well as postdepositional processes such as differential bioturbation and dissolution [Thomas, 2003]. At present, it is unclear whether the offset observed in the sediment record reflects a true time lag, because there are only a few high-resolution isotopic foraminiferal records across the PETM. We do not see such a pattern for the onset of ETM2 (Figure 3). The planktic and benthic isotope records show a coherent pattern, suggesting that the injection of isotopically depleted carbon was rapidly mixed within all oceanic carbon reservoirs (i.e., within the ocean mixing time of  $\sim 10^3$  yr).

[25] In contrast to the PETM, the onset of ETM2 was gradual, and our single-specimen stable isotope analyses of *Acarinina* and *Subbotina* confirm the presence of intermediate carbon isotope values in surface waters during the onset of the ETM2-CIE, as also seen in the single-specimen benthic isotope record at Site 690 [Stap et al., 2010]. The largest unidirectional change in the  $\delta^{13}\text{C}$  record of *Acarinina* occurred during the second transition. The isotopic variation within this interval is too large to estimate the exact rate of change, but the period of transition can be constrained to less than 21 kyr.

## 5. Conclusions

[26] The negative Carbon Isotope Excursion (CIE) during Eocene Thermal Maximum 2 as observed in surface dwelling planktonic foraminifera was  $\sim 1.7\text{‰}$ , slightly more negative than the coeval CIE in the deep sea ( $\sim 1.4\text{‰}$ ). In addition, the estimated oxygen isotope-based SST increase of  $\sim 2^\circ\text{C}$  is significantly less than the  $>3^\circ\text{C}$  increase found for the deep sea. Despite these offsets, the planktic and benthic isotope records show a coherent pattern, suggesting that the injected isotopically depleted carbon was rapidly mixed within all oceanic carbon reservoirs during ETM2, and led to warming of seawater by a few degrees.

[27] The offsets in magnitude between planktic and benthic isotopic records could be due to several factors, such as vital effects, changes in  $[\text{CO}_3^{2-}]$ , partial dissolution and secondary recrystallization, which are difficult to quantify. Environmental causes for the  $\delta^{13}\text{C}$  offsets could be a decline in the biological pump efficiency or increased vertical





mixing, as suggested for the PETM, whereas changes in surface  $\delta^{18}\text{O}_{\text{sw}}$  composition or a seasonal shift in the abundance of the surface dwelling planktonic foraminifera may have caused the  $\delta^{18}\text{O}$  offsets.

## Acknowledgments

[28] We are grateful to two anonymous reviewers and Louis Derry for their constructive comments. This research used samples provided by the Integrated Ocean Drilling Program (IODP). Funding for this research was provided by the Darwin Center for Biogeosciences to L. Stap, NWO ALW investments grant 834.04.003 to L. Lourens, VICI grant 865.06.003 to S. Schouten, and NSF grant OCE 0902959 to E. Thomas. We thank M. Ziegler and G. Ittman for technical support. This is publication DW-2010-1001 of the Darwin Center for Biogeosciences.

## References

- Arenillas, I., E. Molina, and B. Schmitz (1999), Planktic foraminiferal and  $^{13}\text{C}$  isotopic changes across the Paleocene/Eocene boundary at Possagno (Italy), *Int. J. Earth Sci.*, *88*(2), 352–364, doi:10.1007/s005310050270.
- Bemis, B. E., H. J. Spero, D. W. Lea, and J. Bijma (2000), Temperature influence on the carbon isotopic composition of *Globigerina bulloides* and *Orbulina universa* (planktonic foraminifera), *Mar. Micropaleontol.*, *38*(3–4), 213–228, doi:10.1016/S0377-8398(00)00006-2.
- Bijl, P. K., S. Schouten, A. Sluijs, G.-J. Reichert, J. C. Zachos, and H. Brinkhuis (2009), Early Palaeogene temperature evolution of the southwest Pacific Ocean, *Nature*, *461*(7265), 776–779, doi:10.1038/nature08399.
- Cramer, B. S., J. D. Wright, D. V. Kent, and M.-P. Aubry (2003), Orbital climate forcing of  $\delta^{13}\text{C}$  excursions in the late Paleocene–early Eocene (chrons C24n–C25n), *Paleoceanography*, *18*(4), 1097, doi:10.1029/2003PA000909.
- D’Hondt, S., and J. C. Zachos (1998), Cretaceous foraminifera and the evolutionary history of planktic photosymbiosis, *Paleobiology*, *24*(4), 512–523.
- Erez, J., and B. Luz (1983), Experimental paleotemperature equation for planktonic foraminifera, *Geochim. Cosmochim. Acta*, *47*(6), 1025–1031, doi:10.1016/0016-7037(83)90232-6.
- Handley, L., P. N. Pearson, I. K. McMillan, and R. D. Pancost (2008), Large terrestrial and marine carbon and hydrogen isotope excursions in a new Paleocene/Eocene boundary section from Tanzania, *Earth Planet. Sci. Lett.*, *275*(1–2), 17–25, doi:10.1016/j.epsl.2008.07.030.
- Hollis, C. J., et al. (2009), Tropical sea temperatures in the high-latitude South Pacific during the Eocene, *Geology*, *37*(2), 99–102, doi:10.1130/G25200a.1.
- Hönisch, B. (2002), Stable isotope and trace element composition of foraminiferal calcite—From incorporation to dissolution, Ph.D. thesis, Univ. of Bremen, Bremen, Germany.
- Huguet, C., A. Schimmelmann, R. Thunell, L. J. Lourens, J. S. S. Damste, and S. Schouten (2007), A study of the TEX<sub>86</sub> paleothermometer in the water column and sediments of the Santa Barbara Basin, California, *Paleoceanography*, *22*, PA3203, doi:10.1029/2006PA001310.
- Hut, G. (1987), Consultants group meeting on stable isotope reference samples for geochemical and hydrological investigations, Vienna, Austria, report to Director General of the Institute of Atomic Energy Agency, 42 pp., Inst. of At. Energy, Vienna.
- John, C. M., S. M. Bohaty, J. C. Zachos, A. Sluijs, S. J. Gibbs, H. Brinkhuis, and T. J. Bralower (2008), North American continental margin records of the Paleocene–Eocene thermal maximum: Implications for global carbon and hydrological cycling, *Paleoceanography*, *23*, PA2217, doi:10.1029/2007PA001465.
- Kelly, D. C., T. J. Bralower, and J. C. Zachos (1998), Evolutionary consequences of the latest Paleocene thermal maximum for tropical planktonic foraminifera, *Palaeogeogr. Palaeoclimatol. Palaeoecol.*, *141*, 139–161, doi:10.1016/S0031-0182(98)00017-0.
- Kelly, D. C., J. C. Zachos, T. J. Bralower, and S. A. Schellenberg (2005), Enhanced terrestrial weathering/runoff and surface ocean carbonate production during the recovery stages of the Paleocene–Eocene thermal maximum, *Paleoceanography*, *20*, PA4023, doi:10.1029/2005PA001163.
- Kennett, J. P., and L. D. Stott (1991), Abrupt deep-sea warming, palaeoceanographic changes and benthic extinctions at the end of the Paleocene, *Nature*, *353*(6341), 225–229, doi:10.1038/353225a0.
- Kim, J. H., S. Schouten, E. C. Hopmans, B. Donner, and J. S. Sinninghe Damsté (2008), Global sediment core–top calibration of the TEX<sub>86</sub> paleothermometer in the ocean, *Geochim. Cosmochim. Acta*, *72*(4), 1154–1173, doi:10.1016/j.gca.2007.12.010.
- Kim, J. H., J. van der Meer, S. Schouten, P. Helmke, V. Willmott, F. Sangiorgi, N. Koç, E. C. Hopmans, and J. S. Sinninghe Damsté (2010), New indices for calibrating the relationship of the distribution of archaeal isoprenoid tetraether lipids with sea surface temperature, *Geochim. Cosmochim. Acta*, *74*, 4639–4654, doi:10.1016/j.gca.2010.05.027.
- Kroon, D., and G. Ganssen (1989), Northern Indian Ocean upwelling cells and the stable isotope composition of living planktonic foraminifera, *Deep Sea Res., Part A*, *36*(8), 1219–1236.
- Lee, K. E., J.-H. Kim, I. Wilke, P. Helmke, and S. Schouten (2008), A study of the alkenone, TEX<sub>86</sub>, and planktonic foraminifera in the Benguela Upwelling System: Implications for past sea surface temperature estimates, *Geochem. Geophys. Geosyst.*, *9*, Q10019, doi:10.1029/2008GC002056.
- Lourens, L. J., A. Sluijs, D. Kroon, J. C. Zachos, E. Thomas, U. Röhl, J. Bowles, and I. Raffi (2005), Astronomical pacing of late Palaeocene to early Eocene global warming events, *Nature*, *435*, 1083–1087, doi:10.1038/nature03814.
- Luciani, V., L. Giusberti, C. Agnini, J. Backman, E. Fornaciari, and D. Rio (2007), The Paleocene–Eocene Thermal Maximum as recorded by Tethyan planktonic foraminifera in the Forada section (northern Italy), *Mar. Micropaleontol.*, *64*(3–4), 189–214, doi:10.1016/j.marmicro.2007.05.001.
- Nguyen, T. M. P., M. R. Petrizzo, and R. P. Speijer (2009), Experimental dissolution of a fossil foraminiferal assemblage (Paleocene–Eocene Thermal Maximum, Dababiya, Egypt): Implications for paleoenvironmental reconstructions, *Mar. Micropaleontol.*, *73*(3–4), 241–258, doi:10.1016/j.marmicro.2009.10.005.
- Ostlund, H. S., H. Craig, W. S. Broecker, and D. Spencer (1987), *GEOSECS Atlantic, Pacific and Indian Ocean Expeditions*, vol. 7, *Shorebased Data and Graphics*, Natl. Sci. Found., Washington, D. C.



- Pearson, P. N., P. W. Ditchfield, J. Singano, K. G. Harcourt-Brown, C. J. Nicholas, R. K. Olsson, N. J. Shackleton, and M. A. Hall (2001), Warm tropical sea surface temperatures in the Late Cretaceous and Eocene epochs, *Nature*, *413*(6855), 481–487, doi:10.1038/35097000.
- Petrizzo, M. R. (2007), The onset of the Paleocene-Eocene Thermal Maximum (PETM) at Sites 1209 and 1210 (Shatsky Rise, Pacific Ocean) as recorded by planktonic foraminifera, *Mar. Micropaleontol.*, *63*(3–4), 187–200, doi:10.1016/j.marmicro.2006.11.007.
- Petrizzo, M. R., G. Leoni, R. P. Speijer, B. De Bernardi, and F. Felletti (2008), Dissolution susceptibility of some Paleogene planktonic foraminifera from ODP Site 1209 (Shatsky Rise, Pacific Ocean), *J. Foraminiferal Res.*, *38*(4), 357–371, doi:10.2113/gsjfr.38.4.357.
- Pierre, C., C. Vergnaud-Grazzini, and J. C. Faugeres (1991), Oxygen and carbon stable isotope tracers of the water masses in the Central Brazil Basin, *Deep Sea Res., Part A*, *38*(5), 597–606, doi:10.1016/0198-0149(91)90065-N.
- Roberts, C. D., A. N. LeGrande, and A. K. Tripathi (2009), Climate sensitivity to Arctic seaway restriction during the early Paleogene, *Earth Planet. Sci. Lett.*, *286*(3–4), 576–585, doi:10.1016/j.epsl.2009.07.026.
- Schiffelbein, P., and S. Hills (1984), Direct assessment of stable isotope variability in planktonic foraminifera populations, *Palaeogeogr. Palaeoclimatol. Palaeoecol.*, *48*, 197–213, doi:10.1016/0031-0182(84)90044-0.
- Schouten, S., E. Hopmans, E. Shefuß, and J. S. Sinninghe Damsté (2002), Distributional variations in marine crenarchaeotal membrane lipids: A new tool for reconstructing ancient sea water temperatures?, *Earth Planet. Sci. Lett.*, *204*, 265–274, doi:10.1016/S0012-821X(02)00979-2.
- Schouten, S., C. Huguet, E. C. Hopmans, M. V. M. Kienhuis, and J. S. Sinninghe Damsté (2007), Analytical methodology for TEX<sub>86</sub> paleothermometry by high-performance liquid chromatography/atmospheric pressure chemical ionization-mass spectrometry, *Anal. Chem.*, *79*(7), 2940–2944, doi:10.1021/ac062339v.
- Schrag, D. P., D. J. Depaolo, and F. M. Richter (1995), Reconstructing past sea-surface temperatures: Correcting for diagenesis of bulk marine carbonate, *Geochim. Cosmochim. Acta*, *59*(11), 2265–2278, doi:10.1016/0016-7037(95)00105-9.
- Sexton, P. F., P. A. Wilson, and P. N. Pearson (2006), Microstructural and geochemical perspectives on planktic foraminiferal preservation: “Glassy” versus “Frosty,” *Geochem. Geophys. Geosyst.*, *7*, Q12P19, doi:10.1029/2006GC001291.
- Sluijs, A., S. Schouten, T. H. Donders, P. L. Schoon, U. Rohl, G.-J. Reichert, F. Sangiorgi, J.-H. Kim, J. S. Sinninghe Damsté, and H. Brinkhuis (2009), Warm and wet conditions in the Arctic region during Eocene Thermal Maximum 2, *Nat. Geosci.*, *2*(11), 777–780, doi:10.1038/ngeo0668.
- Spero, H. J. (1992), Do planktic foraminifera accurately record shifts in the carbon isotopic composition of seawater  $\Sigma\text{CO}_2$ , *Mar. Micropaleontol.*, *19*(4), 275–285, doi:10.1016/0377-8398(92)90033-G.
- Spero, H. J., J. Bijma, D. W. Lea, and B. E. Bernis (1997), Effect of seawater carbonate concentration on foraminiferal carbon and oxygen isotopes, *Nature*, *390*, 497–500.
- Stap, L., A. Sluijs, E. Thomas, and L. Lourens (2009), Patterns and magnitude of deep sea carbonate dissolution during Eocene Thermal Maximum 2 and H2, Walvis Ridge, southeastern Atlantic Ocean, *Paleoceanography*, *24*, PA1211, doi:10.1029/2008PA001655.
- Stap, L., L. Lourens, E. Thomas, A. Sluijs, S. Bohaty and J. C. Zachos (2010), High-resolution deep-sea carbon and oxygen isotope records of Eocene Thermal Maximum 2 and H2, *Geology*, *38*, 607–610, doi:10.1130/G30777.1.
- Thomas, D. J., T. J. Bralower, and J. C. Zachos (1999), New evidence for subtropical warming during the late Paleocene thermal maximum: Stable isotopes from Deep Sea Drilling Project Site 527, Walvis Ridge, *Paleoceanography*, *14*(5), 561–570, doi:10.1029/1999PA900031.
- Thomas, D. J., J. C. Zachos, T. J. Bralower, E. Thomas, and S. Bohaty (2002), Warming the fuel for the fire: Evidence for the thermal dissociation of methane hydrate during the Paleocene-Eocene thermal maximum, *Geology*, *30*(12), 1067–1070, doi:10.1130/0091-7613(2002)030<1067:WTFTF>2.0.CO;2.
- Thomas, E. (2003), Extinction and food at the seafloor: A high-resolution benthic foraminiferal record across the Initial Eocene Thermal Maximum, Southern Ocean Site 690, *Spec. Pap. Geol. Soc. Am.*, *369*, 319–332.
- Tripathi, A., and H. Elderfield (2004), Abrupt hydrographic changes in the equatorial Pacific and subtropical Atlantic from foraminiferal Mg/Ca indicate greenhouse origin for the thermal maximum at the Paleocene-Eocene Boundary, *Geochem. Geophys. Geosyst.*, *5*, Q02006, doi:10.1029/2003GC000631.
- Uchikawa, J., and R. E. Zeebe (2010), Examining possible effects of seawater pH decline on foraminiferal stable isotopes during the Paleocene-Eocene Thermal Maximum, *Paleoceanography*, *25*, PA2216, doi:10.1029/2009PA001864.
- Zachos, J. C., L. D. Stott, and K. C. Lohman (1994), Evolution of early Cenozoic marine temperatures, *Paleoceanography*, *9*(2), 353–387, doi:10.1029/93PA03266.
- Zachos, J. C., M. W. Wara, S. Bohaty, M. L. Delaney, M. R. Petrizzo, A. Brill, T. J. Bralower, and I. Premoli-Silva (2003), A transient rise in tropical sea surface temperature during the Paleocene-Eocene Thermal Maximum, *Science*, *302*, 1551–1554, doi:10.1126/science.1090110.
- Zachos, J. C., et al. (2004), *Proceedings of the Ocean Drilling Program Initial Reports*, vol. 208, Ocean Drill. Program, College Station, Tex.
- Zachos, J. C., S. Bohaty, C. John, and H. McCarran (2007), The Paleocene-Eocene carbon isotope excursion: Constraints from individual shell planktonic foraminifer records, *Philos. Trans. R. Soc. A*, *365*, 1829–1842, doi:10.1098/rsta.2007.2045.